Inorganic Chemistry

Article

pubs.acs.org/IC

Spectroscopic and Structural Elucidation of Uranium Dioxophenoxazine Complexes

Scott A. Pattenaude,[†] Christopher S. Kuehner,[†] Walter L. Dorfner,[‡] Eric J. Schelter,[‡] Phillip E. Fanwick,[†] and Suzanne C. Bart*[,†]

[†]H.C. Brown Laboratory, Department of Chemistry, Purdue University, West Lafayette, Indiana 47907, United States

[‡]P. Roy and Diana T. Vagelos Laboratories, Department of Chemistry, University of Pennsylvania, Philadelphia, Pennsylvania 19104, United States

Supporting Information

ABSTRACT: Uranium derivatives of a redox-active, dioxophenoxazine ligand, $(DOPO^{q})_2UO_2$, $(DOPO^{sq})UI_2(THF)_2$, $(DOPO^{cat})UI(THF)_2$, and $Cp^*U(DOPO^{cat})(THF)_2$ (DOPO = 2,4,6,8-tetra-*tert*-butyl-1-oxo-1*H*-phenoxazin-9-olate), have been synthesized from U(VI) and U(III) starting materials. Full characterization of these species show uranium complexes bearing ligands in three different oxidation states. The electronic structures of these complexes have been explored using ^{1}H NMR and electronic absorption spectroscopies, and where possible, X-ray crystallography and SQUID magnetometry.

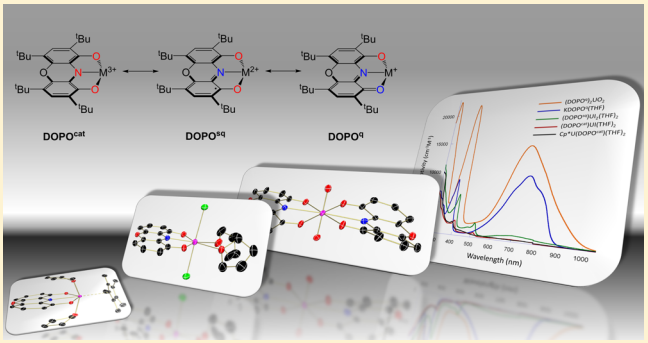

INTRODUCTION

With the recent activity aimed toward understanding redox noninnocent ligands and their cooperative participation in metal mediated transformations, new ligand frameworks have emerged.[1,2] One such class is dioxophenoxazine ligands (DOPO), which have recently been synthesized[3] and studied with transition metals.[4,5] These ligands are an improvement over the related 3,5-di-*tert*-butyl-1,2-quinone-1-(2-oxy-3,5-di-*tert*-butylphenyl)imine frameworks (ONO), as the DOPO class contains an additional ether linkage that introduces rigidity and prevents bending of the π-system needed for electron storage.[6−8] The DOPO ligands are stable in their monoanionic (quinone, $DOPO^{q}$), dianionic (semiquinone, $DOPO^{sq}$), and trianionic (catecholate, $DOPO^{cat}$) forms, potentially serving to stabilize metals while still being capable of mediating multielectron processes (Scheme 1).

Recently, several studies have reported the utility of the bis(DOPO) ligand framework to support transition metals in a variety of oxidation states. Studies by Minkin and co-workers described the synthesis of divalent, first-row transition metal bis(ligand) complexes, $M(DOPO)_2$ (M = Mn, Fe, Co, Ni, Cu, Zn), bearing the monoanionic $DOPO^{q}$ form of the ligand.[5] The manganese, iron, and cobalt derivatives are all high spin, and it is hypothesized that the rigid DOPO framework prevents interconversion between the redox-isomeric forms of the complexes. More recently, Brown and co-workers have shown analogous hexavalent octahedral molybdenum and tungsten bis(ligand) species supported by the fully reduced, trianionic form of the dioxophenoxazine ligand, $DOPO^{cat}$.[4] Interestingly, the chromium analogue shows an unusual electronic structure, one ligand in the reduced semiquinone form, DOPOsq, and the other in the oxidized quinone form, DOPOq, generating a C_{2v} symmetric chromium(III) species, $Cr(DOPO^{q})(DOPO^{sq})$. Despite this recent interest in the DOPO family of ligands, the ability of this framework to support f-block elements has not yet been explored.

The DOPO class of ligands is related to the iminoquinone (^{R}iq)/iminosemiquinone (^{R}isq)/amidophenolate (^{R}ap) (iq = 4,6-di-*tert*-butyl-2-[(R)-iminoquinone]; ap = 4,6-di-*tert*-butyl-2-[(R)-amidophenolate]; R = ^{t}Bu, Ad, dipp; Ad = 1-adamantyl, dipp =2,6-diisopropylphenyl) family, which has recently been used to perform multielectron oxidative addition[9] and reductive elimination on uranium.[10] For instance, the bidentate amidophenolate ligands in $(^{R}ap)_2U(THF)_2$ can mediate oxidative addition of chlorine or iodine at monomeric U(IV) complexes, where the two reducing equivalents necessary for bond cleavage are derived from the ligand. Thus, radical iminosemiquinone ligands (^{R}isq) support the products from oxidative addition, which are dimeric, $[(^{R}isq)_2UCl]_2(\mu\text{-}Cl)_2$, and monomeric, $(^{R}isq)_2UI_2$.[9] Alternately, radical reductive elimination of bibenzyl occurs from tetrabenzyluranium using the iminoquinone form of the ligand. These are subsequently reduced to generate the corresponding amidophenolate uranium dialkyls, $(^{R}ap)U(CH_2Ph)_2$.[10] With this multielectron chemistry at U(IV) established, we sought to explore the reactivity with the DOPO ligand, as it has an additional phenoxy substituent to afford more robust tridentate uranium

Received: April 15, 2015
Published: June 23, 2015

DOI: 10.1021/acs.inorgchem.5b00855
Inorg. Chem. 2015, 54, 6520−6527

Scheme 1. Redox Noninnocence of the DOPO Ligand

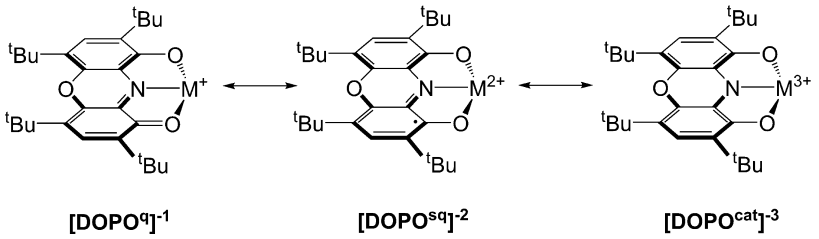

complexes. Herein, we report the synthesis and full characterization of a family of uranium complexes bearing dioxophenoxazine ligands in three different oxidation states.

EXPERIMENTAL SECTION

General Considerations. All air- and moisture-sensitive manipulations were performed using standard Schlenk techniques or in an MBraun inert atmosphere drybox with an atmosphere of purified nitrogen. The MBraun drybox was equipped with a cold well designed for freezing samples in liquid nitrogen as well as two −35 °C freezers for cooling samples and crystallizations. Solvents for sensitive manipulations were dried and deoxygenated using literature procedures with a Seca solvent purification system.[11] Benzene-d_6 and pyridine-d_5 were purchased from Cambridge Isotope Laboratories. Benzene-d_6 was dried with molecular sieves and sodium, and degassed by three freeze−pump−thaw cycles. Pyridine-d_5 was dried with molecular sieves and degassed by three freeze−pump−thaw cycles. 2,4,6,8-Tetra-*tert*-butyl-9-hydroxy-1*H*-phenoxazin-1-one (HDOPO^q),[4] $UO_2[N(SiMe_3)_2]_2(THF)_2$,[12] KCH_2Ph,[13] potassium pentamethylcyclopentadienide (KCp*),[14] $UI_3(THF)_4$,[15,16] and KC_8[17] were prepared according to literature procedures.

^{1}H NMR spectra were recorded on a Varian Inova 300 spectrometer at 299.992 MHz. All chemical shifts are reported relative to the peak for $SiMe_4$, using ^{1}H (residual) chemical shifts of the solvent as a secondary standard. The spectra for paramagnetic molecules were obtained by using an acquisition time of 0.5 s; thus, the peak widths reported have an error of ±2 Hz. For paramagnetic molecules, the ^{1}H NMR data are reported with the chemical shift, followed by the peak width at half height in Hertz, the integration value, and, where possible, the peak assignment. Elemental analyses were performed by Complete Analysis Laboratories, Inc., Parsippany, New Jersey. Electronic absorption measurements were recorded at 294 K in THF in sealed 1 cm quartz cuvettes with a Jasco V-6700 spectrophotometer. Infrared spectra were recorded using a Perkin−Elmer FT-IR Spectrum RX I spectrometer. Samples were made by crushing the solids, mixing with dry KBr, and pressing into a pellet.

Single crystals of Cp*U(DOPO^{cat})(THF)$_2$ (**4**) and (DOPO^{sq})-$UI_2(THF)_2$ (**2**) for X-ray diffraction were coated with poly(isobutene) oil in a glovebox and quickly transferred to the goniometer head of a Nonius KappaCCD image plate diffractometer equipped with a graphite crystal, incident beam monochromator. Preliminary examination and data collection were performed with Mo K_α radiation (λ = 0.71073 Å). A single crystal of $(DOPO^q)_2UO_2$ (**1**) was coated with polybutenes oil in a glovebox and quickly transferred to the goniometer head of a Rigaku Rapid II image plate diffractometer equipped with a MicroMax002+ high intensity copper X-ray source with confocal optics. Preliminary examination and data collection were performed with Cu K_α radiation (λ = 1.54184 Å). Cell constants for data collection were obtained from least-squares refinement. The space groups were identified using the program XPREP.[18] The structures were solved by direct methods using either SIR2004[19] or SHELXT.[20] Refinement was performed on a LINUX PC using SHELX-2013.[20] The data were collected at a temperature of either 150(1) K or 200(1) K.

Solid-state magnetic data were collected using a Quantum Design Multi-Property Measurement System (MPMS-7) warmed from 2−300 K and cooled from 300−2 K at 1 T and at 2 K from 0−7 T. Drinking straws were used to contain the samples for measurement and were dried under a dynamic vacuum overnight before use in an inert atmosphere (N_2) drybox. While empty, a straw was crimped using a hot pair of tweezers to melt it together. The samples were added directly into the crimped straw and were massed to the nearest 0.1 mg using a calibrated and leveled Mettler-Toledo AL-204 analytical balance. Approximately 10.0 mg of quartz wool was added to the straw above the sample to hold it in place. The straw was then crimped above the sample and quartz wool with hot tweezers to complete the seal. The samples, contained in the sealed drinking straws for measurement, were transferred to the MPMS under inert atmosphere and immediately loaded into the inert atmosphere of the measurement chamber with three evacuation/purge cycles. Corrections for the intrinsic diamagnetism of the samples were made using Pascal's constants.[21]

The resonance Raman system was based on SpectraCode optical rail design. A Melles-Griot HeNe laser (632.8 nm, 25 mW) was used as an excitation source. The laser was coupled into a SpectraCode optical rail via an optical fiber. Semrock MaxLine Laser-line and Stopline Single-notch filters were used to select and guide the laser beam through an objective lens (Nikon 100x EPlan, Olympus 20x LMPlanFL and Mitutoyo 50x MPlan) to the sample. A video system was used to choose the sample area for data collection. Backscattered Raman photons were guided through a second fiber into an Acton Research SpectraPro 300i spectrograph (1200 g/mm grating). Spectra were collected as a solution in benzene-d_6 in a sealed cuvette between 300 and 1565 rel. cm^{-1} using Roper Scientific WinbSpec software.

Preparation of KDOPO^q(THF) (KDOPO^q = potassium 2,4,6,8-tetra-*tert*-butyl-1-oxo-1*H*-phenoxazin-9-olate). A 100 mL round-bottom flask was charged with HDOPO^q (1.816 g, 4.15 mmol) and 30 mL of THF, and was cooled to −35 °C. An orange solution of KCH_2Ph (0.544 g, 4.15 mmol) in 15 mL of THF was also cooled to −35 °C and added dropwise to the HDOPO^q solution, causing a color change from violet to dark blue. After stirring for 1 h the volatiles were removed *in vacuo* yielding a blue powder (quantitative yield) assigned as KDOPO^q(THF). A small amount of bibenzyl was noted by ^{1}H NMR analysis, but the product was pure enough to use without further purification. Analysis for $C_{32}H_{46}KNO_4$: Calcd C, 70.16; H, 8.46; N, 2.56. Found C, 69.99; H, 8.39; N, 2.76. ^{1}H NMR (C_6D_6, 25 °C): δ = 1.40 (m, 4H, THF−CH_2), 1.58 (br s, 36H, −C(CH_3)$_3$), 3.54 (m, 4H, THF−CH_2), 7.62 (s, 2H, Ar−C*H*).

Preparation of $(DOPO^q)_2UO_2$ (1). A 20 mL scintillation vial was charged with $UO_2[N(SiMe_3)_2]_2(THF)_2$ (0.050 g, 0.069 mmol) and 5 mL of THF. This orange solution was stirred for 5 min before a solution of HDOPO^q (0.060 g, 0.138 mmol) in 5 mL of THF was added dropwise. The resulting green solution was stirred for 1 h, then the volatiles were removed *in vacuo*. This green powder was taken up in 3 mL of pentane and stirred for 10 min. The solution was then cooled to −35 °C, causing precipitation of a dark-green powder. This was collected by filtration and assigned as $(DOPO^q)_2UO_2$ (0.068 g, 0.059 mmol, 86%). Green crystals suitable for X-ray analysis were grown by slow evaporation from toluene/THF (10:1) overnight at 25 °C. Analysis for $C_{56}H_{76}N_2O_8U$: Calcd C, 58.83; H, 6.70; N, 2.45. Found C, 59.01; H, 6.77; N, 2.62. Raman (C_6D_6, cm^{-1}) 843 (s, U═O symmetric stretch). IR (KBr pellet, cm^{-1}): 2958 (s), 1591 (w), 1498 (s), 1357 (s), 1290 (s), 1253 (s), 1203 (m), 1041 (w), 937 (w, U═O

DOI: 10.1021/acs.inorgchem.5b00855
Inorg. Chem. 2015, 54, 6520−6527

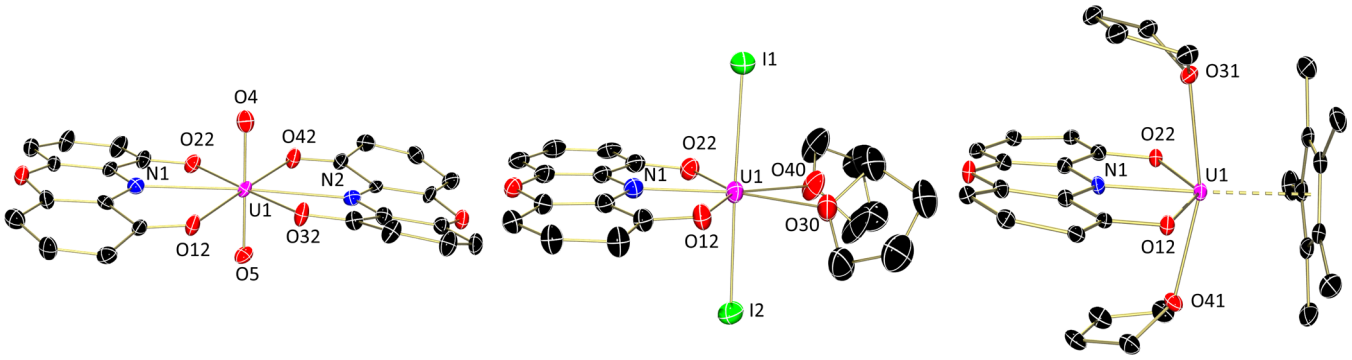

Figure 1. Molecular structures of $(DOPO^{q})_2UO_2$ (**1**) (left), $(DOPO^{sq})UI_2(THF)_2$ (**2**) (center), and $Cp^*U(DOPO^{cat})(THF)_2$ (**4**) (right) shown at 30% probability ellipsoids. Hydrogen atoms, *tert*-butyl groups, and cocrystallized solvent molecules have been omitted for clarity.

asymmetric stretch). ^{1}H NMR (C_6D_6, 25 °C): δ = 1.55 (s, 36H, $-C(CH_3)_3$), 1.93 (s, 36H, $-C(CH_3)_3$), 7.92 (s, 4H, Ar$-CH$).

Preparation of $(DOPO^{sq})UI_2(THF)_2$ (2). A 20 mL scintillation vial was charged with $UI_3(THF)_4$ (0.083 g, 0.091 mmol) and $KDOPO^{q}(THF)$ (0.050 g, 0.091 mmol). To this mixture, 8 mL of diethyl ether were added, and the resulting emerald green solution was stirred for 5 min before it was filtered over Celite. After removing volatiles *in vacuo*, an emerald green powder (0.097 g, 0.090 mmol, 99%) was collected and assigned as $(DOPO^{sq})UI_2(THF)_2$. Green crystals suitable for X-ray analysis were grown by slow evaporation from pentane/toluene (5:1) overnight at 25 °C. Analysis for $C_{36}H_{54}I_2NO_5U$: Calcd C, 40.31; H, 5.07; N, 1.31. Found C, 40.47; H, 5.17; N, 1.47. ^{1}H NMR (C_6D_6, 25 °C): δ = −248.69 (141, 2H, Ar$-CH$), −5.38 (9, 18H, $-C(CH_3)_3$), 37.66 (19, 18H, $-C(CH_3)_3$).

Preparation of $(DOPO^{cat})UI(THF)_2$ (3). A 20 mL scintillation vial was charged with $UI_3(THF)_4$ (0.248 g, 0.273 mmol) and $KDOPO^{q}(THF)$ (0.150 g, 0.274 mmol). To this mixture, 15 mL of diethyl ether were added, and the resulting emerald green solution was stirred for 15 min before it was cooled to −35 °C. A suspension of KC_8 (0.033 g, 0.244 mmol) in 5 mL of ether was also cooled to −35 °C and was added to the emerald green solution dropwise, yielding a dark green solution. After stirring for 15 min, the resulting brown solution was filtered over Celite. Upon removal of volatiles *in vacuo*, a yellow-brown powder was collected (0.240 g, 0.253 mmol, 93%) and assigned as $(DOPO^{cat})UI(THF)_2$. To obtain analytically pure sample the compound was taken up in 10 mL of pentane and stirred for 10 min. This solution was cooled to −35 °C and then filtered. Upon removal of volatiles *in vacuo*, a yellow-brown powder was collected (0.105 g, 0.111 mmol, 41%). Analysis for $C_{36}H_{54}INO_5U$: Calcd C, 45.72; H, 5.76; N, 1.48. Found C, 45.67; H, 5.60; N, 1.59. ^{1}H NMR (C_6D_6, 25 °C): δ = −1.73 (4, 18H, $-C(CH_3)_3$), 15.99 (5, 2H, Ar$-CH$), 36.32 (6, 18H, $-C(CH_3)_3$).

Alternative Preparation of $(DOPO^{cat})UI(THF)_2$ (3). A 20 mL scintillation vial was charged with $(DOPO^{sq})UI_2(THF)_2$ (0.050 g, 0.047 mmol) and 15 mL of diethyl ether. This solution was cooled to −35 °C before KC_8 (0.006 g, 0.047 mmol) was added as a solid. After stirring for 15 min, the resulting brown solution was filtered over Celite. Upon removal of volatiles *in vacuo*, a yellow-brown powder was collected (0.038 g, 0.035 mmol, 74%) and assigned as $(DOPO^{cat})UI(THF)_2$ based on ^{1}H NMR spectroscopic data.

Preparation of $Cp^*U(DOPO^{cat})(THF)_2$ (4). A 20 mL scintillation vial was charged with $UI_3(THF)_4$ (0.300 g, 0.331 mmol), KCp* (0.058 g, 0.331 mmol), and 8 mL of THF. This blue solution was stirred for 3 h before a solution of $KDOPO^{q}(THF)$ (0.181 g, 0.331 mmol) in 6 mL of THF was slowly added. After stirring for 1 min, KC_8 (0.045 g, 0.331 mmol) was added quickly as a solid. This brown solution was stirred for 1 h then filtered over Celite. After removing volatiles *in vacuo*, a brown powder (0.272 g, 0.285 mmol, 86%) was collected and assigned as $Cp^*U(DOPO^{cat})(THF)_2$. Brown crystals suitable for X-ray analysis were grown by slow evaporation from pentane overnight at −35 °C. Analysis for $C_{46}H_{69}NO_5U$: Calcd C, 57.91; H, 7.29; N, 1.47. Found C, 57.76; H, 7.40; N, 1.63. ^{1}H NMR (C_6D_6, 25 °C): δ = −65.83 (7, 8H, THF$-CH_2$), −20.10 (3, 18H, $-C(CH_3)_3$), −9.70 (13, 8H, THF$-CH_2$), 7.20 (4, 15H, Cp*$-CH_3$), 7.57 (4, 2H, Ar$-CH$), 16.52 (4, 18H, $-C(CH_3)_3$).

RESULTS AND DISCUSSION

Our studies commenced with the synthesis of the protonated $DOPO^{q}$ ligand, $HDOPO^{q}$, which was accomplished using a recently improved procedure[4] that differs from the initial synthesis.[3] Deprotonation of purple $HDOPO^{q}$ was accomplished using benzylpotassium at −35 °C and confirmed by ^{1}H NMR spectroscopy (Figure S1, benzene-d_6), which showed overlapping resonances for the two *tert*-butyl groups at 1.58 ppm and signals for the aryl$-CH$ at 7.62 ppm. Two additional resonances (4H each) signify a coordinated THF molecule, making the overall formula, $KDOPO^{q}(THF)$.

With the protonated and deprotonated forms of the ligand in hand, uranium complexes that feature the DOPO ligand in each of its possible oxidation states were planned. To generate a uranium complex with the most oxidized form of the ligand, $DOPO^{q}$, a bis(ligand) uranyl species was targeted. In this case, there are no additional electrons on uranium that can reduce the ligand, thus eliminating ambiguity of ligand oxidation states. Treating an orange toluene solution of $UO_2[N(SiMe_3)_2]_2(THF)_2$[12] with 2 equiv of $HDOPO^{q}$ resulted in a color change to emerald green (eq 1). The concentration of this solution facilitated precipitation of a dark green powder assigned as $(DOPO^{q})_2UO_2$ (**1**) in high yield (86%).

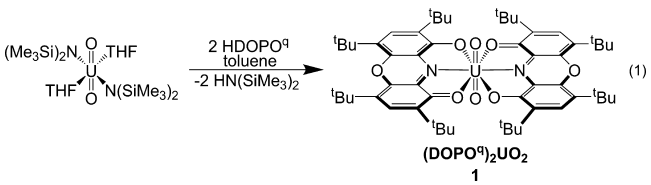

Characterization of **1** by ^{1}H NMR spectroscopy (Figure S2, benzene-d_6) shows a spectrum consistent with a diamagnetic, D_2 symmetric molecule. Two resonances (36H each) for *tert*-butyl groups are visible at 1.55 and 1.93 ppm, as well as a signal for the aryl-CH at 7.92 ppm (4H). Vibrational spectroscopic data supports a U(VI) center in **1**, with a O═U═O absorption at 843 cm^{-1} for the symmetric stretch (Raman) as well as one at 937 cm^{-1} for the asymmetric stretch (infrared). These data are as expected based on other uranyl compounds.[22]

In order to provide baseline structural parameters for the $DOPO^{q}$ ligand, a single crystal of **1** was grown from slow evaporation of a concentrated toluene/THF solution (10:1) at 25 °C and analyzed by X-ray crystallography (Figure 1, bond

DOI: 10.1021/acs.inorgchem.5b00855
Inorg. Chem. 2015, 54, 6520−6527

Scheme 2. Synthesis of DOPO Uranium Complexes

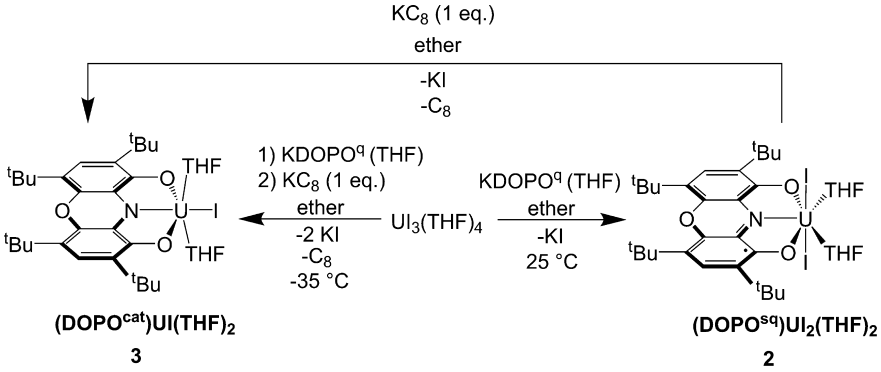

distances in Figure 3). Refinement of the data confirmed the assignment of **1**, showing a molecular structure with two DOPO^{q} ligands *trans* to one another in the plane perpendicular to the uranyl moiety. The solid-state structure shows a pseudohexagonal bipyramidal uranium center, with some distortions from planarity in the DOPO^{q} ligands. This distortion likely relieves steric strain from the *tert*-butyl groups on the *trans* DOPO^{q} ligand. The uranyl U−O bonds of 1.765(4) and 1.768(5) Å are as expected for other uranyl species, including the starting material, $UO_2[N(SiMe_3)_2]_2(THF)_2$.[23]

Previous work has demonstrated that uranium−ligand distances are an accurate gauge for determining the extent of ligand reduction.[24−26] As shown in Scheme 1, the oxidized form of the ligand would have one monoanionic and one dative U−O interaction, which should be delocalized. Thus, the combination of the two resonance structures would produce U−O distances between anionic and dative bonds for uranium, which is observed. The U−O distances of 2.480(4) and 2.518(4) Å (Figure 3) are longer than a typical aryloxide ligand for uranium.[27] The U−N distance of 2.676(6) Å is quite long as compared to a uranium-amide; it is more consistent with a dative uranium−nitrogen bond, as would be expected for the oxidized DOPO^{q} ligand.[27]

The intraligand parameters for **1** also support the idea that the DOPO ligand is in the quinone oxidation state. For instance, the C−O distances of 1.273(7) and 1.261(7) Å are elongated from C═O double bonds due to the resonance contribution. Similarly, the C−N bond lengths of 1.335(7) and 1.344(7) Å are the same within error. These parameters are on the order of those observed for Pb(DOPO^{q})$_2$, which has C−O distances of 1.297(4) and 1.246(4) Å and C−N distances of 1.347(4) and 1.316(4) Å.[4] Similarly, Minkin reports values for Mn(DOPO^{q})$_2$ through Zn(DOPO^{q})$_2$ with C−O values that range from 1.266(2) to 1.294(5) Å and C−N distances from 1.315(1) to 1.333(5) Å.[5] These structural parameters measured for the ligands in **1** were used to determine the metrical oxidation states (MOS) as established by Brown and coworkers for the DOPO ligand, which is useful due to the sensitivity of this method for the degree of π bonding in a molecule.[4] Applying that model to **1** gave an MOS value of −1.25(19), which is consistent with other reports describing the quinone form of the ligand, including Pb(DOPO^{q})$_2$ (MOS = −1.06(15)).[4] Accordingly, the assignment of a hexavalent uranyl with two monoanionic DOPO^{q} ligands is well supported by crystallographic and spectroscopic data.

Low-valent derivatives of the DOPO ligand were also attempted by metalation with trivalent $UI_3(THF)_4$. Previously, treating $UI_3(THF)_4$ with the related iminoquinone ligand, ^{R}iq, resulted in electron transfer from the uranium to the ligand, forming the uranium(IV) iminosemiquinone product, (^{R}isq)-$UI_3(THF)_2$ (R = dipp), as confirmed by magnetometry experiments.[10] Given the similarities between the iminoquinone and the dioxophenoxazine frameworks, it is hypothesized that the analogous uranium oxidation event will occur for the dioxophenoxazine complexes as well. In this case, addition of one equivalent of blue KDOPO^{q}(THF) to a blue diethyl ether suspension of $UI_3(THF)_4$ at −35 °C (Scheme 2) produced an emerald green powder following workup. Analysis by ^{1}H NMR spectroscopy (Figure S3, benzene-d_6) shows a paramagnetically broadened and shifted spectrum, indicative of a C_{2v} symmetric molecule. Two resonances (18H each) for the *o*- and *p*-*tert*-butyl groups appear at −5.38 and 37.66 ppm, respectively, along with a smaller resonance (2H) shifted drastically to −248.69 ppm for the aryl−C*H* protons. This extreme upfield shift has been noted previously for uranium species bearing radical ligands,[26,28,29] leading to the assignment of the green product as (DOPO^{sq})UI_2, with a semiquinone radical ligand by analogy to (^{R}isq)$UI_3(THF)_2$.

No THF resonances were noted in the ^{1}H NMR spectrum, likely due to dissociation/association of labile THF ligands on the NMR time scale. This hypothesis was tested by addition of pyridine-d_5 to an NMR tube containing a known amount of (DOPO^{sq})UI_2 (Figure S4, benzene-d_6). Immediately, resonances for uncoordinated THF were apparent, indicating ligand substitution was operative. Quantification of the liberated THF was possible by integration against a mesitylene internal standard. This experiment established the presence of two equivalents of THF for each equivalent of (DOPO^{sq})UI_2, leading to the more accurate assignment of (DOPO^{sq})-$UI_2(THF)_2$ (**2**).

Confirmation for the assignment of **2** was obtained by X-ray diffraction of a single crystal grown from slow evaporation of a concentrated pentane solution with several drops of toluene at 25 °C. Refinement revealed a pentagonal bipyramidal uranium species with two iodide ligands and two THF molecules, in addition to the DOPO ligand (Figure 1, structural parameters in Figure 3). The idealized C_{2v} symmetry of **2** in the solid state is consistent with the solution structure as determined by ^{1}H NMR spectroscopy. The U−O distances of 2.203(4) and 2.231(4) Å are significantly contracted from those in **1**, pointing toward ligand reduction as indicated by the shorter U−O distance that is *not* expected for the larger uranium(IV) center. These distances are consistent with those for uranium(IV)−aryloxide interactions.[30] Accordingly, the U−N bond distance has also decreased (2.371(4) Å), but it is still in the

DOI: 10.1021/acs.inorgchem.5b00855
Inorg. Chem. 2015, 54, 6520−6527

range for a U(IV)-amide.[26,30,31] The intraligand distances corroborate a higher degree of reduction as compared to **1**, with C−O distances (1.350(6) and 1.355(6) Å) that are elongated by ∼0.1 Å, in agreement with single bond character that is expected for the iminosemiquinone resonance structure shown in Scheme 1. The corresponding C−N bonds are very similar to those in **1**, showing that they are less sensitive to ligand oxidation state changes. Accordingly, the iminosemiquinone ligand in Cr(DOPO^{q})(DOPO^{sq}) has respective C−O and C−N averages of 1.335(2) and 1.349(2) Å. Thus, the ligand in **2** is most consistent with a U(IV) center ligated by a dianionic DOPO^{sq} ligand. The calculated MOS value of −2.67(21) for the DOPO ligand in **2** suggests a higher degree of reduction in the ligand than predicted by the U−N and U−O distances. Based on the U(IV) assignment, the U−O$_{THF}$ and U−I distances are as expected compared to UI$_4$(1,4-dioxane)$_2$.[15]

To further corroborate the presence of the iminosemiquinone in **2**, self-consistent solid-state magnetic measurements of two independently prepared, analytically pure samples were performed (Figure 2). The room temperature moment of 2.87

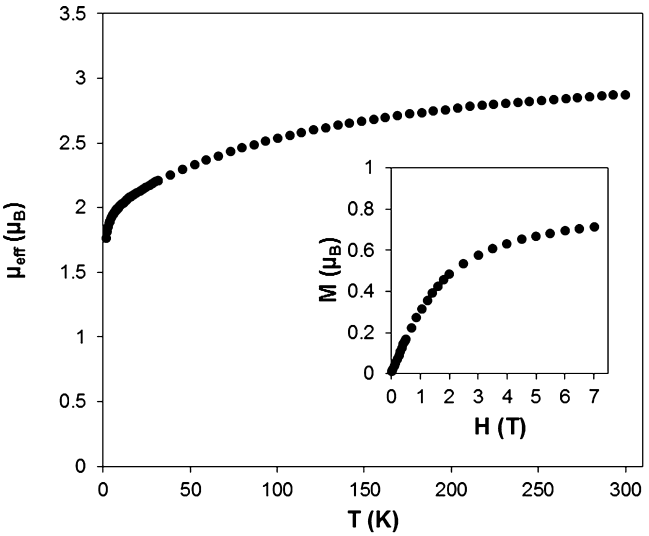

Figure 2. Variable temperature molar magnetic data for **2** collected between 300 and 2 K at 1 T. The inset is a plot of variable field data collected at 2 K.

μ_B was consistent with reported magnetic data for uranium(IV) complexes with ligand radicals.[25,32] It is well established that μ_{eff} decreases monotonically with temperature in the cases of U(IV) cations in low symmetry ligand fields, due to the depopulation of the nine ligand field levels for the ion.[33−35] The data for **2** showed this type of behavior, consistent with its assignment as a uranium(IV) complex (Figure 2). The low temperature effective magnetic moment of **2** was determined to be 1.81 μ_B (2 K), which was close to the expected spin-only moment predicted for a ligand based doublet (1.73 μ_B, assuming g = 2.0).[36] The U(IV) ion is also well-established to have a singlet ground state in low symmetry ligand fields.[37,38] The assignment of a magnetic singlet U(IV) ion and ligand-based doublet for **2** is consistent with the observed moment, where the low temperature contributions approach zero for the uranium(IV) cation and 1.73 μ_B for the ligand radical. Field-dependent data were measured at 2 K and achieved a limit at 0.79 μ_B at 7 T, which also supported assignment of a single ligand-based unpaired electron per molecule. An alternate interpretation of the magnetic data for **2** would be assignment of a catecholate-DOPO ligand in a trianionic, closed shell form, coordinated to a J = 5/2 uranium(V) cation: (DOPO^{cat})-U(V) as the ground state. In this scenario, the uranium would retain paramagnetism at low temperature, consistent with the low temperature and field dependent responses for **2**. However, the room temperature moment for **2** does not support (DOPO^{cat})-U(V) because the observed moment of 2.87 μ_B at 300 K is significantly larger than those typically observed for uranium-(V) complexes.[38] Overall the magnetic measurements were most consistent with a configuration of **2** comprising S = 1/2 DOPO$^{sq\bullet}$ radical and a 5f^2 U(IV) singlet at low temperature: (DOPO^{sq})$^{\bullet}$-U(IV).

The synthesis of a uranium species bearing the most reduced form of the ligand, DOPO^{cat}, was attempted by performing the same reaction as for the synthesis of **2** but with an equivalent of potassium graphite (KC_8), which afforded a yellow-brown powder (Scheme 2). As in the case for **2**, ^{1}H NMR spectroscopic analysis (Figure S5, benzene-d_6) showed a C_{2v} symmetric molecule with two resonances at −1.73 and 36.32 ppm for the *tert*-butyl groups on the ligand; however, in this case the C*H* protons for the DOPO aryl groups appeared at 15.99 ppm, indicating loss of radical character. With the addition of an external reductant, the product was assigned as (DOPO^{cat})UI bearing a triply reduced catecholate ligand. By charge balance considerations, a U(IV) ion is hypothesized.

No THF resonances were noted in the ^{1}H NMR spectrum for (DOPO^{cat})UI, again likely due to dissociation/association of labile THF ligands on the NMR time scale. Once again, addition of pyridine-d_5 to (DOPO^{cat})UI caused THF dissociation (Figure S6, benzene-d_6). Quantification by integration (mesitylene internal standard) showed two equivalents of THF were present for each equivalent of (DOPO^{cat})UI; thus, the more accurate assignment is as (DOPO^{cat})UI(THF)$_2$ (**3**). Compound **3** could also be generated by addition of KC_8 to **2** (Scheme 2). Unfortunately, difficulty in obtaining single crystals precluded characterization of **3** by X-ray diffraction.

To circumvent the crystallization issues for **3**, the pentamethylcyclopentadienyl analogue, Cp*U(DOPO^{cat})-(THF)$_2$ (**4**), was synthesized. Addition of KDOPO^{q}(THF) to *in situ* generated Cp*UI$_2$(THF)$_3$,[39] followed immediately by one equivalent of KC_8, generated the desired product as a brown solid after workup (eq 2). Characterization by ^{1}H NMR

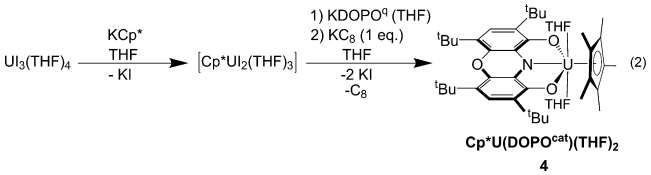

spectroscopy (Figure S7, benzene-d_6) showed a C_{2v} symmetric molecule, with resonances for the *tert*-butyl protons at −20.10 and 16.52 ppm, along with a resonance at 7.20 ppm assignable to the Cp*−C*H*$_3$ protons. The aryl−C*H* resonance appeared close to this at 7.57 ppm, which is on the order of that found for **3** (15.99 ppm). This is in contrast to compound **2**, where the aryl−C*H* resonance appears at −248.69 ppm, pointing to the absence of a ligand radical in **4**.

Brown crystals of **4** were obtained from a concentrated pentane solution at −35 °C and analyzed by X-ray crystallography. The molecular structure features a uranium

DOI: 10.1021/acs.inorgchem.5b00855
Inorg. Chem. 2015, 54, 6520−6527

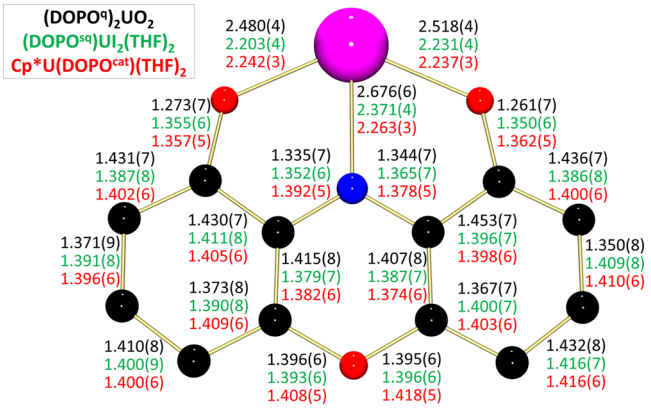

Figure 3. Bond distance comparison (Å) for $(DOPO^{q})_2UO_2$ (**1**), $(DOPO^{sq})UI_2(THF)_2$ (**2**), and $Cp^*U(DOPO^{cat})(THF)_2$ (**4**).

with the DOPO and Cp* ligands in a *trans* arrangement (Figure 1, structural parameters in Figure 3). Two THF molecules lie perpendicular to the DOPO ligand plane and are *trans* with respect to each other. The solid state structure shows the THF rings are bent away from the Cp* ring, presumably relieving steric interactions. The U−Cp^*_{cent} distance of 2.493 Å is on the order of those for other U(IV)−Cp* complexes.[26,31,40] As in the case for **2**, the U−O distances (2.237(3) and 2.242(3) Å) point to anionic uranium−oxygen bonds, as would be expected for a reduced ligand framework. Divergent from **2**, however, is the U−N distance of 2.263(3) Å, which is 0.1 Å shorter, and reflective of a uranium-amide linkage[31] resulting from a further degree of reduction. The intraligand C−O distances of 1.357(5) and 1.362(5) Å are indistinguishable from those in **2**, once again supporting a reduced ligand. However, the C−N distance of 1.392(5) Å is statistically longer than those in **2**, as would be consistent with C−N single bonds and consistent with the $DOPO^{cat}$ resonance structure. The corresponding distances for $Mo(DOPO^{cat})_2$ and $W(DOPO^{cat})_2$, which have been established to contain trianionic catecholate ligands, have C−O average distances of 1.366(6) and 1.376(4) Å, respectively, which match well with those in **4**.[4] The average C−N distances for these transition metal analogues of 1.362(9) and 1.372(4) Å are within error of those for the uranium species, **4**. This structural support and the similar spectroscopic properties of **3** and **4** point to a trianionic $DOPO^{cat}$ ligand in both cases. This is supported by the value obtained for **4** using the MOS model (−2.87(16)), which is on the order of those for $Mo(DOPO^{cat})_2$ (−2.83(23), −2.60(18)) and $W(DOPO^{cat})_2$ (−3.00(22), −2.80(19)).

Further confirmation for the oxidation states of complexes **1**−**4** was gathered using electronic absorption spectroscopy (Figure 4). Data in the UV−visible regions for the DOPO uranium series and $KDOPO^{q}(THF)$ showed intense absorptions throughout the UV region, as has been noted previously.[3,4] Striking differences are found in the visible region, which shows an absorption for $KDOPO^{q}(THF)$ at 735 nm with a high molar absorptivity (9,750 cm^{-1} M^{-1}) similar to what was observed for the corresponding sodium salt (λ_{max} = 695 nm).[3] For the uranium complexes, **1** shows a strong $\pi-\pi^*$ absorption at 719 nm with a high molar absorptivity (14,400 cm^{-1} M^{-1}). This large absorbance is characteristic of a transition into an empty $DOPO^{q}$ -based π^* orbital. For compound **2**, there is a much weaker (ε = 874 cm^{-1} M^{-1}) $\pi-\pi^*$ absorption noted at 704 nm, assigned as a transition into the half-filled π^* orbital of $DOPO^{sq}$. In the case of this uranium semiquinone species, the molar absorptivity is significantly lower than that reported for transition metal and main group semiquinone complexes.[7,41] However, the previously established trend for these complexes shows a larger molar absorptivity for the quinone ligands and a lower molar absorptivity for the semiquinone form. While our absolute value for **2** is different than those for transition metal and main group examples, the data still follows this general trend. These bands are absent in complexes **3** and **4**, confirming the closed shell $DOPO^{cat}$ ligand with a filled π^* orbital. Data obtained in the NIR region for **2**−**4** show sharp but weak f−f transitions consistent with U(IV), f^2 centers (Figure 4). For **1**, no peaks

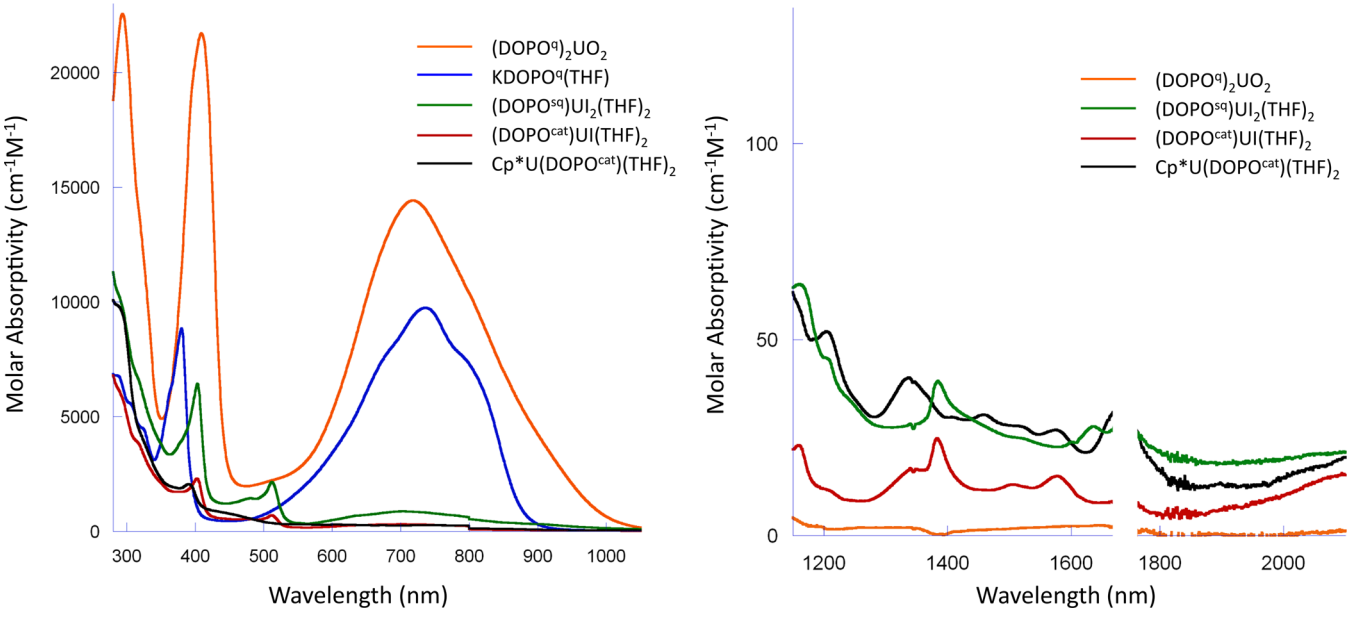

Figure 4. Electronic absorption spectra in the UV/visible region (left) and NIR region (right) for the DOPO series collected as solutions in THF at ambient temperature.

DOI: 10.1021/acs.inorgchem.5b00855
Inorg. Chem. 2015, 54, 6520−6527

are noted in the NIR region, indicating the absence of f–f transitions, which would be expected for a U(VI), f^0 center.

CONCLUSIONS

A series of dioxophenoxazine uranium complexes, $(DOPO^{q})_2UO_2$, $(DOPO^{sq})UI_2(THF)_2$, $(DOPO^{cat})UI(THF)_2$, and $Cp^*U(DOPO^{cat})(THF)_2$, have been synthesized in high yield and characterized. Data obtained using ^{1}H NMR spectroscopy, electronic absorption spectroscopy, X-ray crystallography, and SQUID magnetometry suggest that **1** contains two monoanionic $DOPO^{q}$ ligands at a U(VI) center, while **2** has a dianionic $DOPO^{sq}$ chelate and a U(IV) center. Both **3** and **4** feature a trianionic $DOPO^{cat}$ framework, also ligated to a U(IV) center. Ligand oxidation states were also established by using the intraligand bond distances as determined by X-ray crystallography to calculate the Metrical Oxidation State (MOS) of each ligand.[4] These calculations supported, within error, the assignments of the ligand oxidation states based on experimental data as compared to previously established examples with transition metals.[4,5] Near-infrared absorption data support that the uranium center is tetravalent for **2**–**4** and maintains its +6 oxidation state for **1**. The dioxophenoxazine uranium species described here are exciting new additions to the collection of known uranium species bearing redox active ligands, as the oxygen donor atoms make the DOPO ligand a strong chelator for the oxophilic uranium center. Future studies will be aimed at the utility of these complexes for multielectron transformations.

ASSOCIATED CONTENT

Supporting Information

^{1}H NMR spectroscopic data, X-ray crystallographic experimental details, and cif data. The Supporting Information is available free of charge on the ACS Publications website at DOI: 10.1021/acs.inorgchem.5b00855.

AUTHOR INFORMATION

Corresponding Author

*E-mail: sbart@purdue.edu.

Notes

The authors declare no competing financial interest.

ACKNOWLEDGMENTS

The authors gratefully acknowledge funding from the Division of Chemical Sciences, Geosciences, and Biosciences, Office of Basic Energy Sciences of the U.S. Department of Energy through Grants DE-AC02-12ER16328 (S.C.B.) and DE-SC0006518 (E.J.S.).

REFERENCES

(1) Stang, S.; Lebkuecher, A.; Walter, P.; Kaifer, E.; Himmel, H.-J. *Eur. J. Inorg. Chem.* **2012**, *2012*, 4833–4845.
(2) Guerro, M.; Pham, N. H.; Massue, J.; Bellec, N.; Lorcy, D. *Tetrahedron* **2008**, *64*, 5285–5290.
(3) Olekhnovich, L. P.; Lyubchenko, S. N.; Simakov, V. I.; Shif, A. I.; Kurbatov, S. V.; Lesin, A. V.; Borodkin, G. S.; Ivakhnenko, E. P.; Zhdanov, Y. A. *Dokl. Akad. Nauk* **1999**, *369*, 632–638.
(4) Ranis, L. G.; Werellapatha, K.; Pietrini, N. J.; Bunker, B. A.; Brown, S. N. *Inorg. Chem.* **2014**, *53*, 10203–10216.
(5) Ivakhnenko, E. P.; Starikov, A. G.; Minkin, V. I.; Lyssenko, K. A.; Antipin, M. Y.; Simakov, V. I.; Korobov, M. S.; Borodkin, G. S.; Knyazev, P. A. *Inorg. Chem.* **2011**, *50*, 7022–7032.
(6) Hananouchi, S.; Krull, B. T.; Ziller, J. W.; Furche, F.; Heyduk, A. F. *Dalton Trans.* **2014**, *43*, 17991–18000.
(7) Szigethy, G.; Shaffer, D. W.; Heyduk, A. F. *Inorg. Chem.* **2012**, *51*, 12606–12618.
(8) Wong, J. L.; Sanchez, R. H.; Logan, J. G.; Zarkesh, R. A.; Ziller, J. W.; Heyduk, A. F. *Chem. Sci.* **2013**, *4*, 1906–1910.
(9) Matson, E. M.; Opperwall, S. R.; Fanwick, P. E.; Bart, S. C. *Inorg. Chem.* **2013**, *52*, 7295–7304.
(10) Matson, E. M.; Franke, S. M.; Anderson, N. H.; Cook, T. D.; Fanwick, P. E.; Bart, S. C. *Organometallics* **2014**, *33*, 1964–1971.
(11) Pangborn, A. B.; Giardello, M. A.; Grubbs, R. H.; Rosen, R. K.; Timmers, F. J. *Organometallics* **1996**, *15*, 1518–1520.
(12) Andersen, R. A. *Inorg. Chem.* **1979**, *18*, 209–209.
(13) Schlosser, M.; Hartmann, J. *Angew. Chem., Int. Ed.* **1973**, *12*, 508–509.
(14) Tonzetich, Z. J.; Eisenberg, R. *Inorg. Chim. Acta* **2003**, *345*, 340–344.
(15) Monreal, M. J.; Thomson, R. K.; Cantat, T.; Travia, N. E.; Scott, B. L.; Kiplinger, J. L. *Organometallics* **2011**, *30*, 2031–2038.
(16) Clark, D. L.; Sattelberger, A. P. *Inorg. Synth.* **1997**, *31*, 307–315.
(17) Chakraborty, S.; Chattopadhyay, J.; Guo, W.; Billups, W. E. *Angew. Chem., Int. Ed.* **2007**, *46*, 4486–4488.
(18) Sheldrick, G. M. *Acta Crystallogr.* **2008**, *112*, A64.
(19) Burla, M. C.; Caliandro, R.; Camalli, M.; Carrozzini, B.; Cascarano, G. L.; De Caro, L.; Giacovazzo, C.; Polidori, G.; Spagna, R. *J. Appl. Cryst.* **2005**, *38*, 381–388.
(20) Sheldrick, G. M. *Beta program*.
(21) Bain, G. A.; Berry, J. F. *J. Chem. Educ.* **2008**, *85*, 532.
(22) Berthet, J.-C.; Siffredi, G.; Thuery, P.; Ephritikhine, M. *Chem. Commun.* **2006**, 3184–3186.
(23) Arnold, P. L.; Patel, D.; Blake, A. J.; Wilson, C.; Love, J. B. *J. Am. Chem. Soc.* **2006**, *128*, 9610–9611.
(24) Cladis, D. P.; Kiernicki, J. J.; Fanwick, P. E.; Bart, S. C. *Chem. Commun.* **2013**, *49*, 4169–4171.
(25) Anderson, N. H.; Odoh, S. O.; Yao, Y.; Williams, U. J.; Schaefer, B. A.; Kiernicki, J. J.; Lewis, A. J.; Goshert, M. D.; Fanwick, P. E.; Schelter, E. J.; Walensky, J. R.; Gagliardi, L.; Bart, S. C. *Nat. Chem.* **2014**, *6*, 919–926.
(26) Kiernicki, J. J.; Newell, B. S.; Matson, E. M.; Anderson, N. H.; Fanwick, P. E.; Shores, M. P.; Bart, S. C. *Inorg. Chem.* **2014**, *53*, 3730–3741.
(27) Castro-Rodriguez, I.; Meyer, K. *Chem. Commun.* **2006**, 1353–1368.
(28) Kraft, S. J.; Fanwick, P. E.; Bart, S. C. *Inorg. Chem.* **2010**, *49*, 1103–1110.
(29) Zi, G.; Jia, L.; Werkema, E. L.; Walter, M. D.; Gottfriedsen, J. P.; Andersen, R. A. *Organometallics* **2005**, *24*, 4251–4264.
(30) Meyer, K.; Bart, S. C. *Adv. Inorg. Chem.* **2008**, *60*, 1–30.
(31) Graves, C. R.; Schelter, E. J.; Cantat, T.; Scott, B. L.; Kiplinger, J. L. *Organometallics* **2008**, *27*, 5371–5378.
(32) Anderson, N. H.; Odoh, S. O.; Williams, U. J.; Lewis, A. J.; Wagner, G. L.; Lezama Pacheco, J.; Kozimor, S. A.; Gagliardi, L.; Schelter, E. J.; Bart, S. C. *J. Am. Chem. Soc.* **2015**, *137*, 4690–4700.
(33) Castro-Rodriguez, I.; Olsen, K.; Gantzel, P.; Meyer, K. *J. Am. Chem. Soc.* **2003**, *125*, 4565–4571.
(34) Lewis, A. J.; Williams, U. J.; Kikkawa, J. M.; Carroll, P. J.; Schelter, E. J. *Inorg. Chem.* **2012**, *51*, 37–39.
(35) Lewis, A. J.; Williams, U. J.; Carroll, P. J.; Schelter, E. J. *Inorg. Chem.* **2013**, *52*, 7326–7328.
(36) Castro-Rodriguez, I.; Nakai, H.; Zakharov, L. N.; Rheingold, A. L.; Meyer, K. *Science* **2004**, *305*, 1757–1760.
(37) Boudreaux, E. A.; Mulay, L. N. *Theory and Applications of Molecular Paramagnetism*; Wiley: New York, 1976; p 510.
(38) Kindra, D. R.; Evans, W. J. *Chem. Rev.* **2014**, *114*, 8865–8882.
(39) Avens, L. R.; Burns, C. J.; Butcher, R. J.; Clark, D. L.; Gordon, J. C.; Schake, A. R.; Scott, B. L.; Watkin, J. G.; Zwick, B. D. *Organometallics* **2000**, *19*, 451–457.
(40) Kiernicki, J. J.; Fanwick, P. E.; Bart, S. C. *Chem. Commun.* **2014**, *50*, 8189–8192.

DOI: 10.1021/acs.inorgchem.5b00855
Inorg. Chem. 2015, 54, 6520–6527

(41) Szigethy, G.; Heyduk, A. F. *Dalton Trans.* **2012**, *41*, 8144−8152.

DOI: 10.1021/acs.inorgchem.5b00855
Inorg. Chem. 2015, 54, 6520−6527